IITRI

IIT Research Institute

GPO PRICE $ _____

CSFTI PRICE(S) $ _____

Hard copy (HC) _____
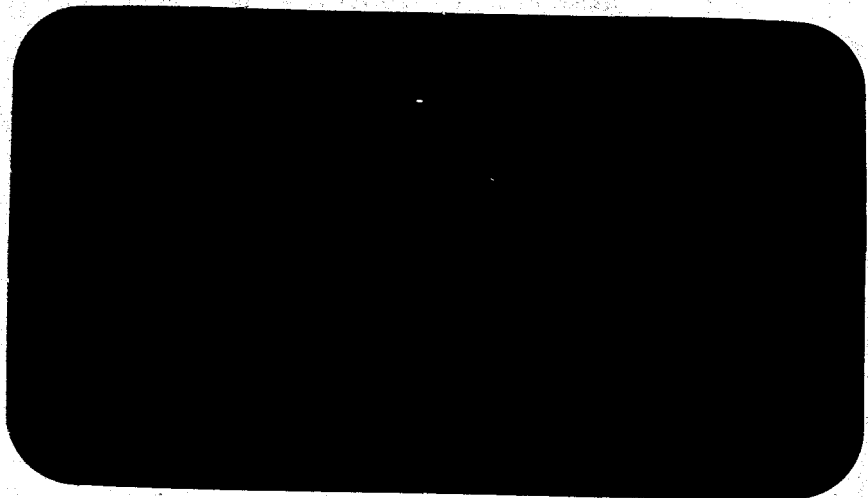
Microfiche (MF) _____

ff 653 July 65

Report No. IITRI-C6018-15
(Quarterly Report)

INVESTIGATION OF LIGHT SCATTERING
IN HIGHLY REFLECTING PIGMENTED COATINGS

National Aeronautics
and Space Administration

IIT RESEARCH INSTITUTE

Report No. IITRI-C6018-15
(Quarterly Report)

INVESTIGATION OF LIGHT SCATTERING
IN HIGHLY REFLECTING PIGMENTED COATINGS

May 1 to August 1, 1965

Contract No. NASr-65(07)
IITRI Project C6018

Prepared by

G. A. Zerlaut, B. H. Kaye,
S. Katz, and V. Raziunas

of

IIT RESEARCH INSTITUTE
Technology Center
Chicago, Illinois 60616

to

National Aeronautics and Space Administration
Office of Advanced Research and Technology
Washington 25, D. C.

Copy No. 8

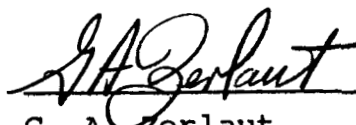August 9, 1965

IIT RESEARCH INSTITUTE

FOREWORD

This is Report No. IITRI-C6018-15 (Quarterly Report) of

IITRI Project C6018, Contract No. NASr-65(07), entitled

"Investigation of Light Scattering in Highly Reflecting Pigmented

Coatings." This report covers the period from May 1 to August

1, 1965. Previous Quarterly Reports were issued on October

11, 1963 (IITRI-C6018-3), January 29, 1964 (IITRI-C6018-6),

May 5, 1964 (IITRI-C6018-8), September 5, 1964 (IITRI-C6018-11),

December 21, 1964 (IITRI-C6018-12), March 10, 1965 (IITRI-C6018-

13), and May 13, 1965 (IITRI-C6018-14).

Major contributors to the program include G. A. Zerlaut,

project leader; Dr. S. Katz and Dr. B. H. Kaye, theoretical

analyses; H. Iglarsh, preparation of random models; and V.

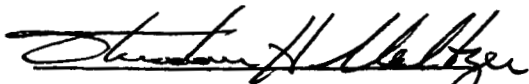Raziunas, experimental investigator.

Respectfully submitted,

IIT RESEARCH INSTITUTE

G. A. Zerlaut
Group Leader

Approved by:

T. H. Meltzer, Manager
Polymer Research

GAZ/am/jb

IIT RESEARCH INSTITUTE

ii

ABSTRACT

33255

The objective of this program is the application of light scattering theories to highly pigmented coatings. The program is aimed at the maximization of the reflection of solar radiation. The adaptation of classical Mie theory to multiple scattering has been extended to different refractive indicies using the radial scattering data of Lowan. The concentrations of 1-micron particles and film thicknesses required to attenuate an incident source to 1% was caluclated. The random-walk investigations involve a descritpion of random intercepts of a circle, the development of the concept of randomly superimposed screens, and preliminary studies of a Monte Carlo approach to the simulation of sections through paint films. It is shown by the use of randomly superimposed screens that a body composed of 50% solids will permit only 0.7% of the incident light to pass through 7 equivalent screens. The implications of this concept are discussed. The experimental studies during this period resulted in the generation of an equation which relates reflectance to the thickness of pigmented films:

$$\frac{1}{100-R_\lambda} = c_2 t^{c_1}$$

where R_λ is the spectral reflectance at wavelength λ, t is the thickness and c_1 and c_2 are constants applicable at wavelength λ.

Author

IIT RESEARCH INSTITUTE

iii

TABLE OF CONTENTS

LIST OF FIGURES

INVESTIGATION OF LIGHT SCATTERING
IN HIGHLY REFLECTING PIGMENTED COATINGS

I. INTRODUCTION

The objective of this program is the application of light-scattering theories to polydisperse, highly reflecting, highly pigmented coatings. The program is aimed at a definition of light-scattering parameters associated with the maximum reflection of solar radiation.

Work thus far has involved (1) a review of light-scattering theory with emphasis on that portion holding the most promise for application to multiple scattering events, (2) the conception of theoretical approaches and random-walk techniques with which to treat the problem of multiple scattering, and (3) the generation of data concerning the optical properties of carefully prepared arrays of silver halide particles dispersed in gelatin.

The adaptation of classical Mie theory to multiple scattering was continued by extending the analysis of the model system discussed in the previous quarterly report (IITRI-C6018-14) to refractive indices of 1.33, 1.44, 1.55, and 2.00 in a medium.

The random-walk investigation discussed in this report includes a description of random intercepts of a circle, the properties of randomly superimposed screens, and preliminary studies of a Monte Carlo approach to the simulation of sections through paint films. Three methods of constructing random intercepts of a circle are presented, and future studies will

IIT RESEARCH INSTITUTE

1

involve the use of these techniques to caluclate the amount of absorption occurring in random paths through pigment particles. The concept of randomly superimposed screens was developed for the purpose of studying the reflectance of paint films. The concept involves the simulation of light through a paint film. An analogous extension of this technique may permit the simulation of sections through composite bodies of various volume concentrations and containing various particle sizes.

Several sets of monodisperse films of silver bromide of various particle thicknesses were prepared. It was found that the thickness and the reflectance are related by an exponential relationship; the optical properties of films containing flocculated dispersions were also investigated.

II. APPLICATION OF CLASSICAL THEORY TO MULTIPLE SCATTERING

This discussion continues the analysis of light scattering of particles by the application of Mie theory to particulate arrays. In the previous report (IITRI-C6018-14) a procedure was proposed for estimating the attenuation of light in a particulate film. The method was applied to particles with real refractive indices, and it was assumed that in a film the scatter of the embedded particles in the foward direction was limited by the angle of total reflection of the film. At the surface of energizing light, all light outside this angle is back scattered. Thus the limits imposed by the angle of total reflection would appear to be of value in determining

the attenuation of light by particles suspended in a film.

In the application of this method, it must be noted that the refractive index of the particles is referred to the surrounding medium, which is the film material. The critical angle for total reflection is a function of the refractive index of the film in its surrounding medium, i.e., air or vaccuum. In the example discussed in the previous report, the critical angle of the film was 45°, and spherical particles of 1-μ radius had a refractive index of 1.44 in the medium. Here the effect of changing the refractive index of the particles and leaving all other parameters unchanged is discussed. Thus:

Angle of total reflection is 45°

Forward-scattering cone subtends 1.84 steradians

Particle radius is 1 μ.

The maximum scattering cases, in which m = 1.33, 1.55, and 2.00, is examined by using the radial scattering data of Lowan.[1] The case in which m = 1.44 is also reviewed.

Conditions for maximum scatter as a function of the parameter $\alpha = 2 \pi r / \lambda$ have been given by LaMer and Sinclair.[2] For the cases indicated, the conditions shown in Table 1 apply.

---

[1]Lowan, A. N., "Tables of Scattering Functions for Spherical Particles," National Bureau of Standards Applied Mathematics Series No. 4., Washington, D.C., 1948.

[2]LaMer, V. and Sinclair, D., Chem. Rev., 44, 245, 1949.

IIT RESEARCH INSTITUTE

Table 1

CONDITIONS FOR MAXIMUM SCATTERING
BY 1-μ TRANSPARENT PARTICLES

Refractive Index m	Maximum Scattering Cross Section K	$\alpha = 2\pi r/\lambda$	λ,m
1.33	3.9	6.3	1.0
1.44*	4.0	4.8	1.31
1.55	4.4	3.6	1.74
2.00	5.2	2.4	2.62

*The data of report No. IITRI-C6018-14 were recalculated from comparison in the present series.

The radial scattering intensity is given by

$$I_\theta = \frac{I_0 \lambda^2 (i_1 + i_2)}{8\pi^2} \tag{1}$$

where I_0 is the incident energy per unit area, and I_θ is the scattered intensity per unit solid angle. The terms i_1 and i_2 are the angular distribution functions for the two plane polarized components scattered by a transparent particle illuminated by incoherent light of wavelength λ.

By using Lowan's data, the scattered intensities in the forward directed cone of 90° included angle were integrated numerically by minimizing the average intensities of the scattered light in the 10° zones between 0° and 50°. These scattered intensities correspond to the $i_1 + i_2$ term of Equation 1 and can be applied in Equation 1 to determine the fraction of

IIT RESEARCH INSTITUTE

incident energy if scattered into the forward cone. By comparison with the total scattering cross section, the backscatter for one particle is determined, and the attenuation, K_a, can be determined as a function of the particle's true cross section. All these calculations have been made and are tabulated in Table 2.

The attenuation cross sections, K_a, are then used to determine the concentration needed to attenuate an incident source by a standard amount. A multiple array of particles that do not interfere with each other is assumed.

The attenuation of a number of particles is given by

$$I = I_0 e^{-K_a \cdot \pi r^2 N} \tag{2}$$

where I is the intensity of the emergent beam. All other terms have been defined previously. Equation 2 is conveniently stated in the form

$$2.303 \log I_0/I = K_a \pi r^2 N \tag{2a}$$

For a given attenuation, N is determined when the appropriate values are assigned to K_a and r. By using the data of Table 2 and assigning a value of 100 to I_0/I, i.e., attenuating the source to 1%, the values shown in Table 3 are obtained.

The tabulated data emphasize the increased attenuation efficiency of particles with high refractive indices.

Table 2

SCATTERING PROPERTIES OF 1-μ PARTICLES
OF VARIOUS REFRACTIVE INDICES AT WAVELENGTHS
CORRESPONDING TO MAXIMUM SCATTERING CROSS SECTIONS

Refractive Index (m)	Scattering Cross-Section (K)	λ, μ	$i_1 + i_2$	I_f x 10^8	Total Scattered Intensity, x 10^8	Backscatter Intensity, x 10^8	Attenuation Cross Section (Ka)
1.33	3.9	1.0	440	10.2	12.3	2.1	0.67
1.44	4.0	1.3	260	10.3	12.6	2.3	0.73
1.55	4.4	1.7	155	10.9	13.8	2.9	0.92
2.00	5.2	2.6	43	6.9	16.4	9.5	3.0

Table 3

CONCENTRATIONS OF 1-μ PARTICLE AND FILM THICKNESSES REQUIRED
TO ATTENUATE THE INCIDENT SIGNAL TO 1%

Refractive Index (m)	Attenuation Cross Section (Ka)	Particle Radius μ	Particles/cm^2 (N)	Film Thickness,* mm
1.33	0.67	1	2.2 x 10^8	2
1.44	0.73	1	2.0 x 10^8	2
1.55	0.92	1	1.46 x 10^8	1.5
2.00	2.00	1	7.3 x 10^7	0.7

*Film thickness for an idealized system of noninterfering particles spaced 10 μ apart.

IITRI-C6018-15

III. RANDOM-WALK TECHNIQUE FOR THE STUDY OF MULTIPLE SCATTERING

A. Random Intercepts of a Circle

The term random as used in everday speech, describes a system that is not uniform or is nonsystematic. When the term is used to describe a system that has finite dimensions in space, it is necessary to be very specific about the exact nature of the randomness of the system considered. Two similar systems can both be random in the technical sense and yet have different physical properties. This fact can be illustrated by considering the problem of drawing random lines across a circle. This situation arises in the study of the light-scattering behavior of paint films, since the average length of intercepts of a circle represents the average path of photons through a spherical pigment particle.

One method of constructing random intercepts of circles is to draw a circle on a piece of paper and then toss thin wires onto the paper in a random manner. The record of the different positions in which the wires fall would then provide a set of random intercepts. However, it can be shown that this kind of randomness is not necessarily a true simulation of the random paths through a spherical object.

There are three possible mathematical procedures for constructing random intercepts. In the first method the perimeter is divided into a convenient set of intervals. Each interval is then allocated a number. To construct a random intercept,

two numbers within the appropriate range are selected from random number tables, and a line is drawn between the two corresponding points on the perimeter. This method is illustrated in Figure 1, and an example of this type of random intercept is shown in Figure 2. Circular graph paper with the perimeter divided into 360 intervals (polar graph paper) was used. Random numbers between 1 and 360 were selected, and 20 random lines drawn to construct the system of random intercepts given in Figure 2.

In the second method for constructing the random lines, the length of a radial line r_1, is chosen from random number tables, and the direction of this line with respect to some fixed direction, θ, is also chosen at random. Then the intercept is drawn perpencircular to this radius. The method is also illustrated in Figure 1. An example of the system is given in Figure 3. Figures 2 and 3 show that shorter intercepts are more probable in method 1, and for that kind of randomness, the average intercept length is small in method 1 than in method 2.

A third method of constructing the random intercepts is to specify a point on the intercept by using a rectangular grid system superimposed upon the circle. Then the direction of the line at this point is selected at random. This is method 3 in Figure 1. In fact, method 3 is equivalent to method 2, since in method 2 all values of direction are equally probable and all values of P are equally probable.

IITRI-C6018-15
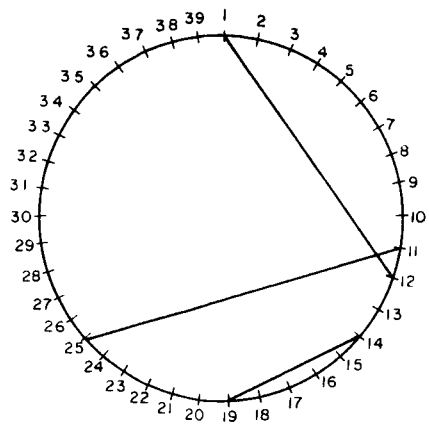
Method 1   Intercept Drawn Between Two Randomly
            Selected Points on the Perimeter
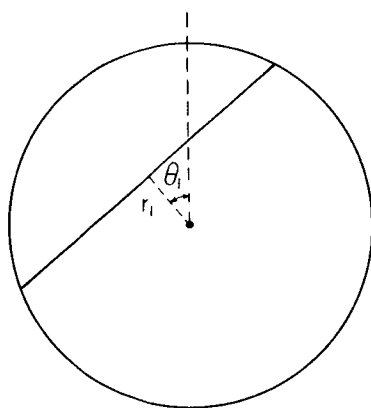
Method 2   Line Drawn Perpendicular to Radius r_1
            at Angle θ_1 to Fixed Direction; r_1 and θ
            Selected Randomly
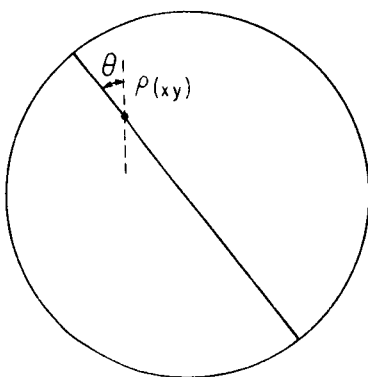
Method 3   Line Drawn Through Point P of Co-Ordinates
            x, y in a Direction θ. The Co-Ordinates
            x and y are on a Rectangular Grid; x, y
            and θ are Selected at Random

FIG. 1   THREE METHODS OF DRAWING RANDOM INTERCEPTS IN
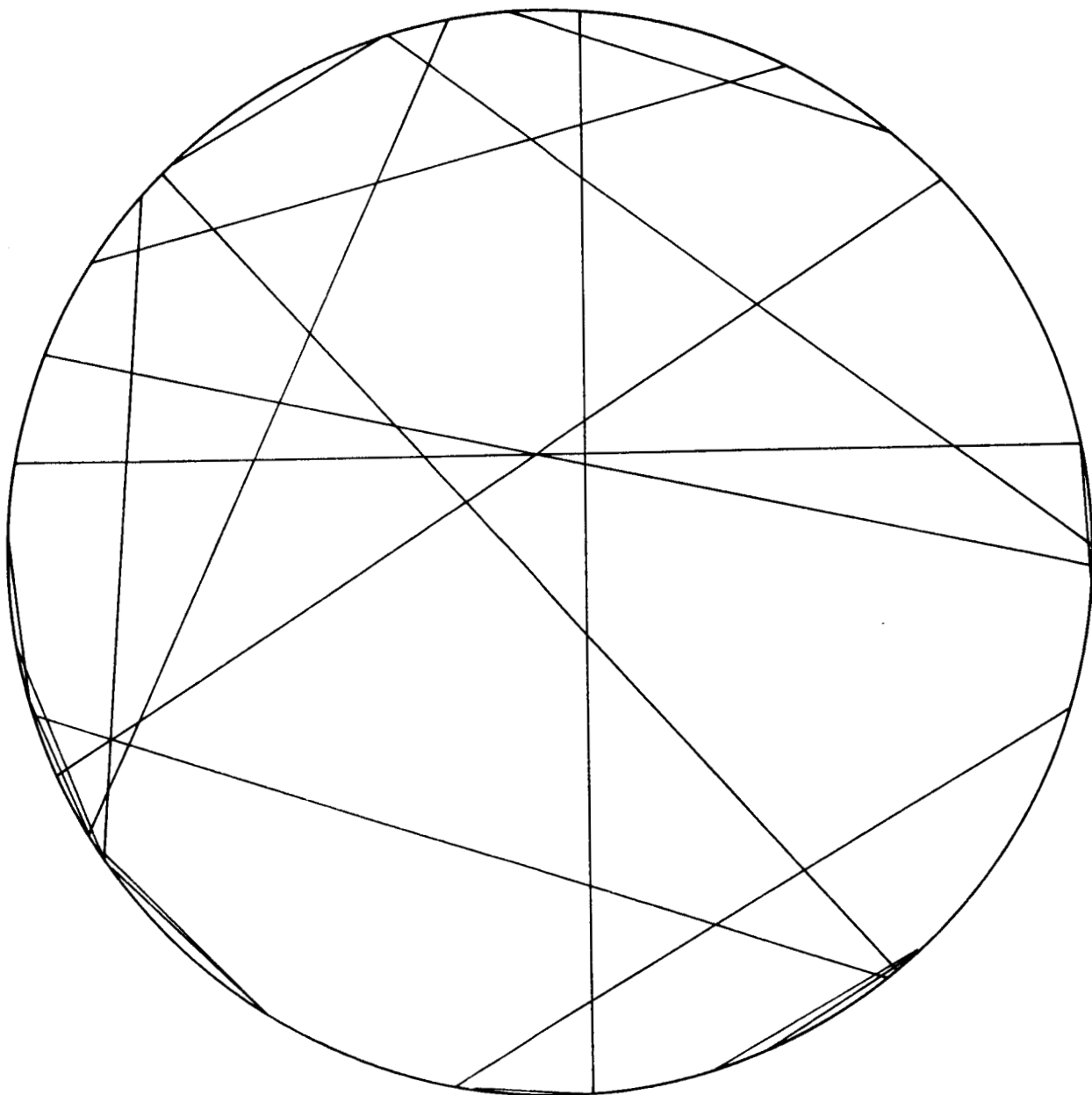   A CIRCLE

FIG. 2 LINES DRAWN BETWEEN RANDOM NUMBERS SELECTED
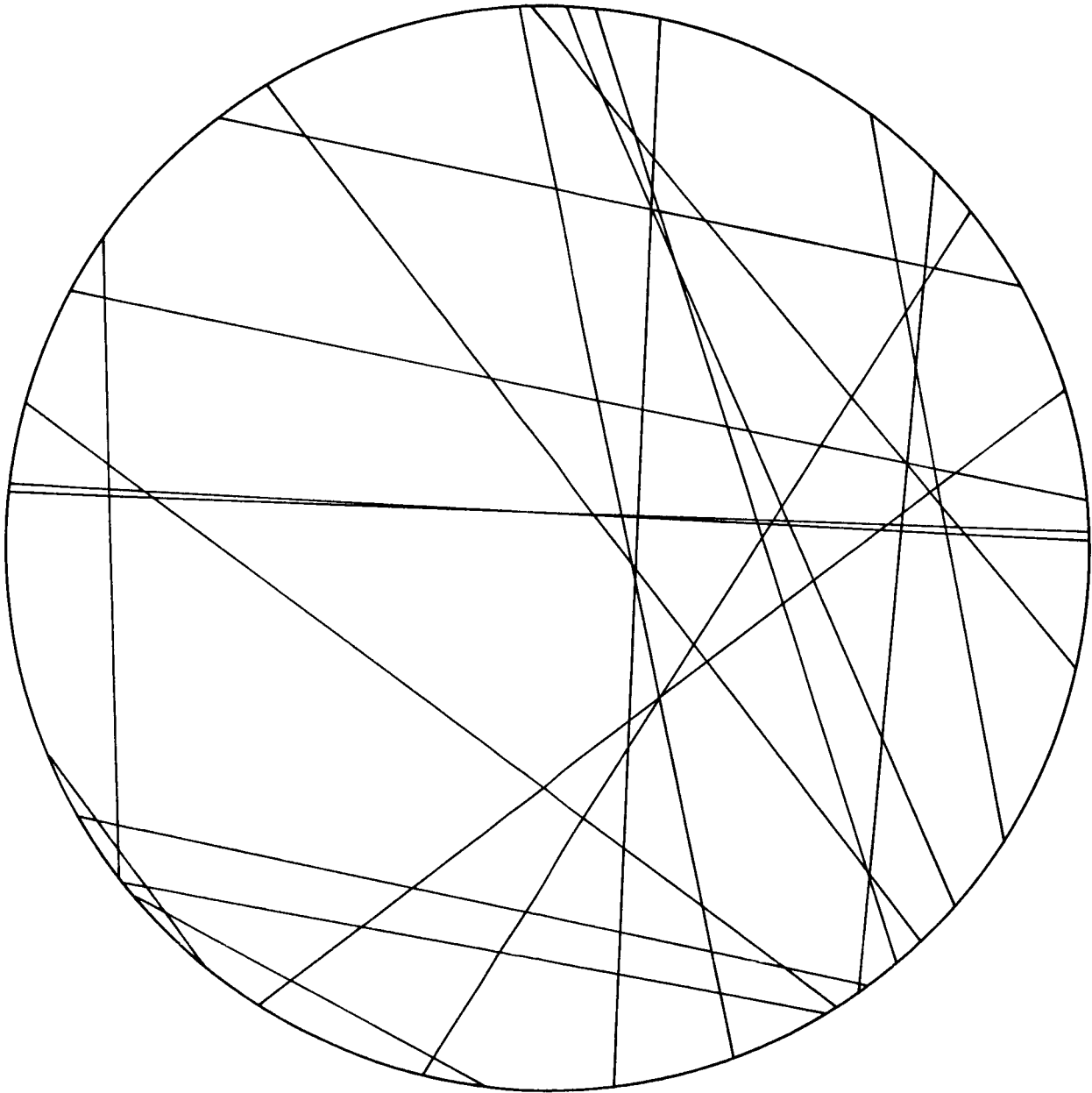ON THE PERIMETER OF A CIRCLE

FIG. 3   LINES DRAWN PERPENDICULAR TO RADIUS FOR RANDOMLY
SELECTED ANGLES TO A FIXED DIRECTION

Consider the families of intercepts for a given direction of various values of r; since each value of r is equally probable, a set of parallel lines will be obtained. Therefore, all possible intercepts are formed by rotating a set of parallel lines about the center point. As the lines come closer and closer together, at any point in space there will be a group of intersecting lines that are spread uniformly through 360°C. This result is also obtained when many intercepts are drawn by method 3. An alternative viewpoint is that x and y specify a value, P, and that corresponding values of r and θ in method 2 will result in an intercept of the same length and direction as choosing x, y, and θ.

The physical method of constructing the random intercepts described at the beginning of this section corresponds to method 2. That is, if we consider the midpoint of the wire tossed onto the paper, the probability of finding this point at any point within the circle is the same for all possible points. This is equivalent to saying that all possible x and y coordinates for this fixed reference point on the wire are equally probable. On landing, all possible orientations of the wire are equally probable; therefore the tossing of the wire onto the circle is physically equivalent to method 2.

Therefore the wire tossing method would give average intercept lengths that correspond to those obtained graphically by using method 2. Now the problem is to decide which method of random intercept construction corresponds to reality in the

IITRI-C6018-15

case of random penetration of a spherical object, and then to deduce a figure for the average path within the sphere for many random events. This figure could then be used to calculate the amount of absorption in random paths through pigment particles. Eventually, it will be necessary to consider the modifications necessary for the consideration of nonspherical particles. Work on these studies is in progress.

B. Some Properties of Random Systems: Randomly Superimposed Screens

It may be possible to study the reflectance of paint films by considering that the penetration of light through the paint film is physically the same as the penetration of light through randomly superimposed screens. In this physical model the pigment particles define the absorbing portions of the screen.

An important property of randomly superimposed screens is the resulting residual area, when viewed exactly perpendicular to the plane of the screen. This is important in determining the direct penetration of an incident beam of light when diffraction of light at the opening of the screens is negligible.

Consider an area, A, within which two laminae, or areas, a_1 and a_2, can be placed at random (Figure 4). To define randomness in this situation, the position of the centroid of each subarea (i.e., a_1 and a_2) is specified by x and y corrdinates, which are selected by using random number tables. A fixed direction on the lamina permits random orientation, i.e., all directions are equally probable. If the whole of the area, A,
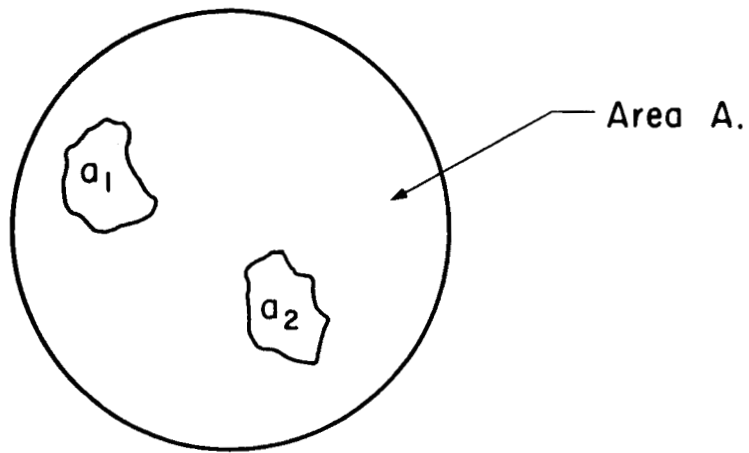
IIT RESEARCH INSTITUTE

FIG. 4   RANDOM LAMINAE WITHIN A DEFINED AREA

is covered with N points equidistant from each other, the number
of points within a_1 is

$$N \times \frac{a_1}{A}$$

The number of points within a_2 is

$$N \times \frac{a_2}{A}$$

If one point within A is selected, the chance that it lies with-
in either area is

$$\frac{a_1}{A} \text{ and } \frac{a_2}{A}$$

The chance that one point will lie within both areas simultane-
ously is

$$\frac{a_1 \times a_2}{A^2}$$

If many events are considered, the average number of points that
will lie in both areas is

$$N \left(\frac{a_1 \times a_2}{A^2} \right)$$

Therefore the average overlap area over many events is

$$\left(\frac{a_1 \times a_2}{A^2} \right) A$$

If A is taken to be unity and a_1 and a_2 are expressed as fractions of unit area, f_1 and f_2, then the fractional area of overlap for many events is $f_1 \times f_2$.

This discussion has proceeded in terms of many superpositions of two areas within a test area. Mathematically, an extended screen with many random apertures of average fractional area, f_1, placed above another screen contains many random apertures of of average fractional area, f_2, which is equivalent to many random superpositions of the two isolated areas.

Physically, the difference is that in the case of the two screens the average is for many events distributed in space, and while in the case of the two areas, the average is for many events distributed in time. Therefore the average residual exposure for two random screens superimposed should be $f_1 \times f_2$. Similarly, for a series of screens it should be $f_1 \times f_2 \times f_3 \cdots f$ for n screens.

Two regular screens superimposed at random should be a close approximation to random screens placed on top of each other. Therefore the following experiment was devised to test the reasoning given in the foregoing discussion. Consider the screen shown in Figure 5. This screen was chosen to fit the proportions of the wire openings in a 325-mesh screen -- the width of the closed protions to the openings was 36/44. The basic unit of the screen is an open portion 44 units square, with opaque portions 36 x 80 units along two sides. Therefore the fractional opening in the screen is
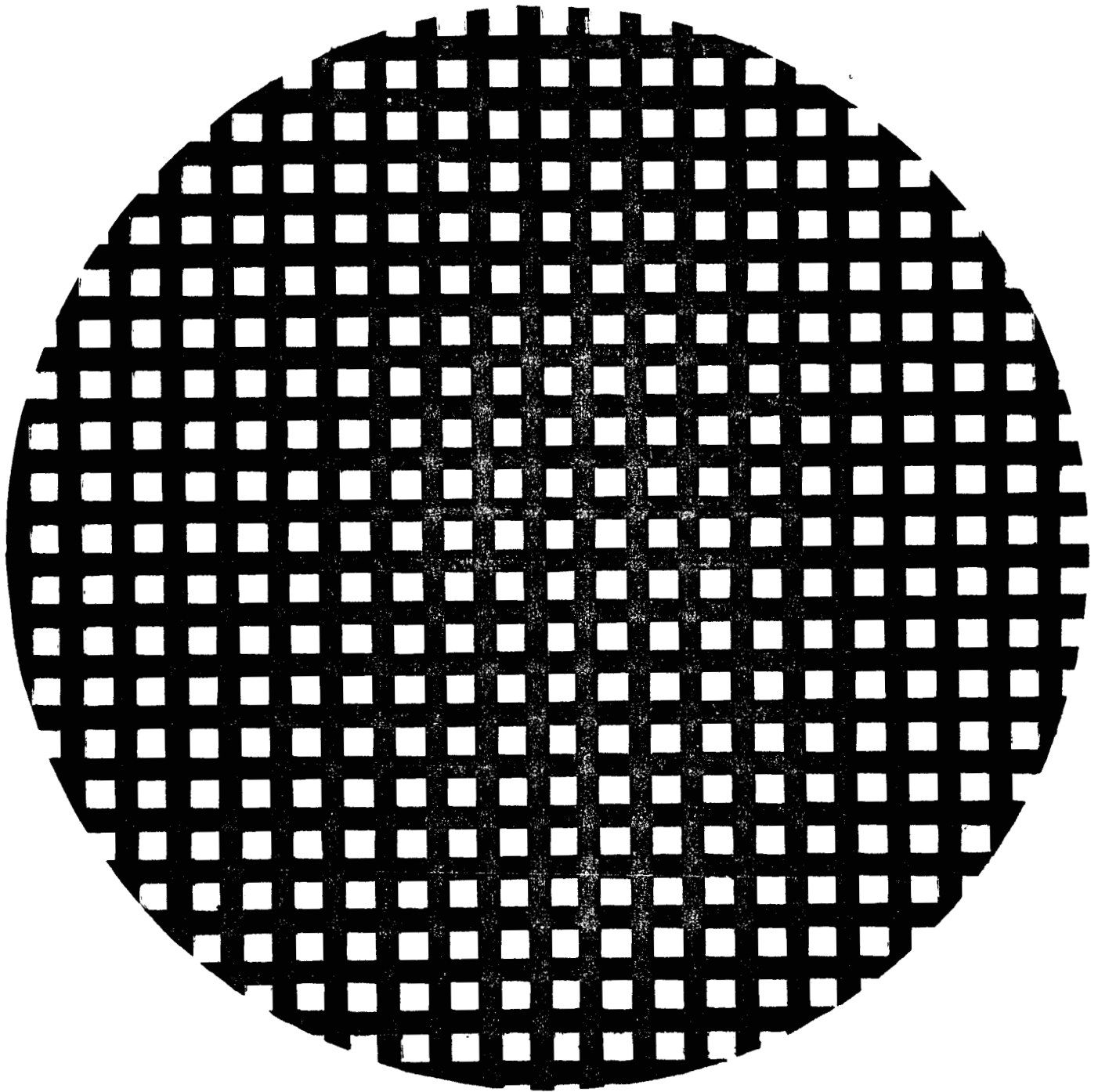
FIG. 5   BASIC SCREEN (OPEN AREA 0.303)

$$\frac{44^2}{80^2} = 0.303$$

Therefore when two screens are superimposed, the open area is 0.092, and for three screens 0.028. A master circular grid (Figure 5) containing 325 whole square openings was constructed on paper. The opaque portions were covered with india ink, and the openings were cut out with a scalpel. This master was copied by Xerography. The master was then superimposed at random on this copy, and the combination again copied by Xerography. The openings common to both screens could be seen clearly on this copy. To measure the open area, the portions of the disk corresponding to the common open area were cut out by using the scalpel. The loss in fractional weight of the disk represents the fraction of open area remaining. The experiment was repeated five times, and the measured fractional openings were: 0.098, 0.105, 0.102, 0.092, and 0.101.

Considering the small number of squares involved and the method of evaluating the common area, these results can be considered to strongly indicate the validity of the reasoning used in predicting a value of 0.092. The disks obtained by the two superimpositions are shown in Figures 6 through 10. The result of superimposing the original master screen randomly on one of the double screens is shown in Figure 11. Again, the common open areas of all three screens were estimated by cutting away the appropriate portions of the reporduced disk and measuring
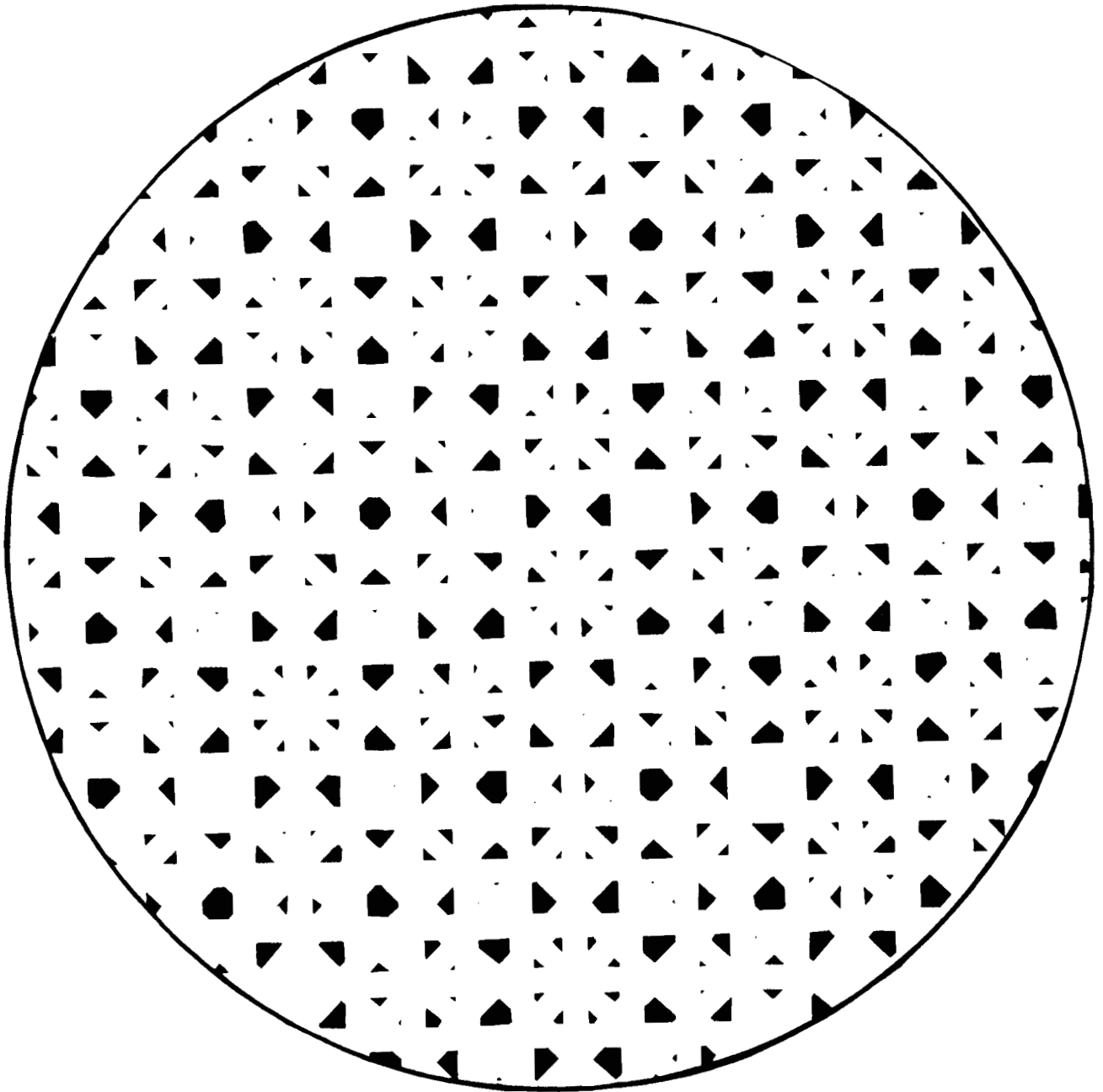
IIT RESEARCH INSTITUTE

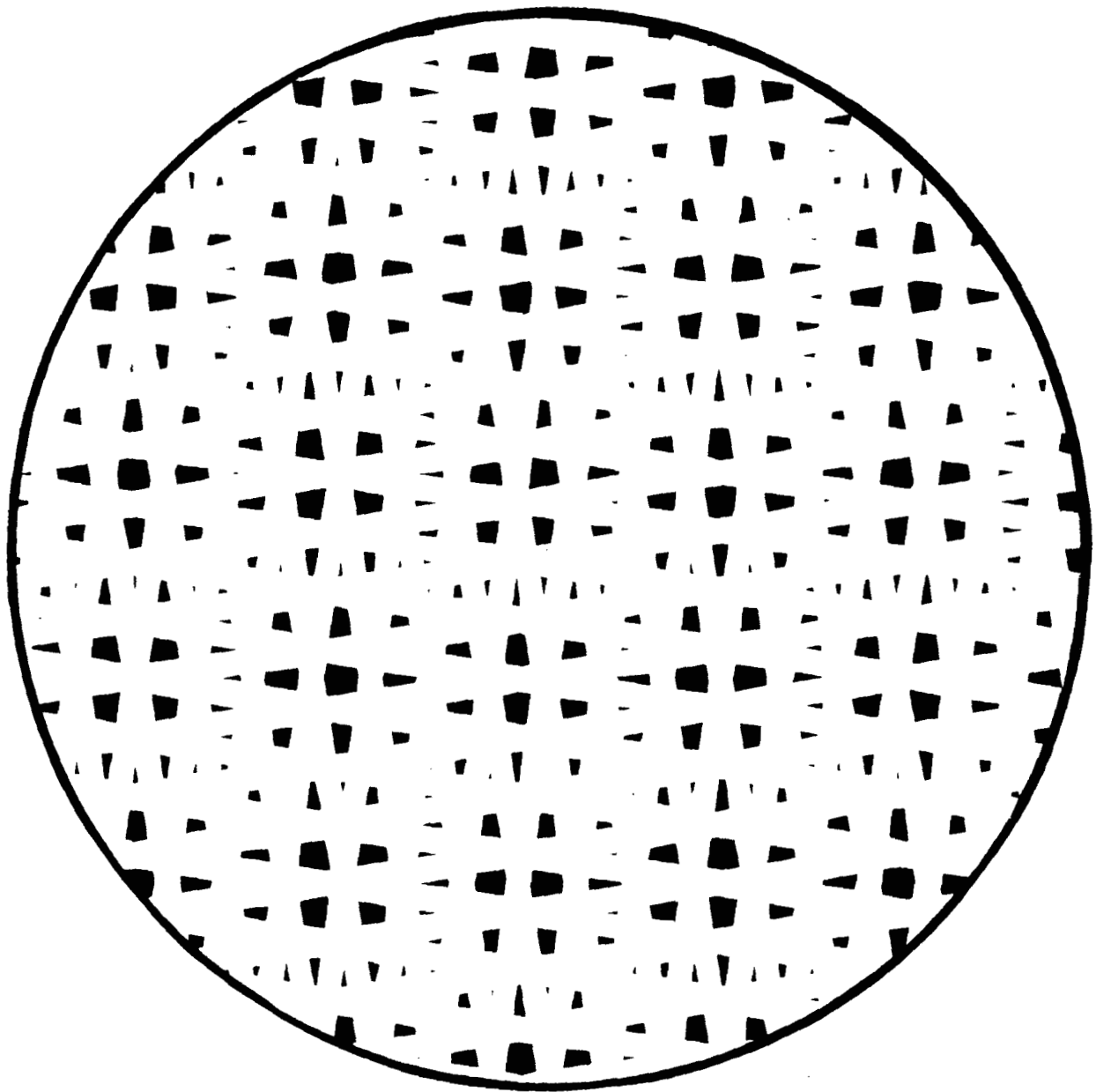FIG. 6 TWO RANDOMLY SUPERIMPOSED SCREENS (OPEN AREA, 0.098)

FIG. 7 TWO RANDOMLY SUPERIMPOSED SCREENS (OPEN AREA, 0.105)
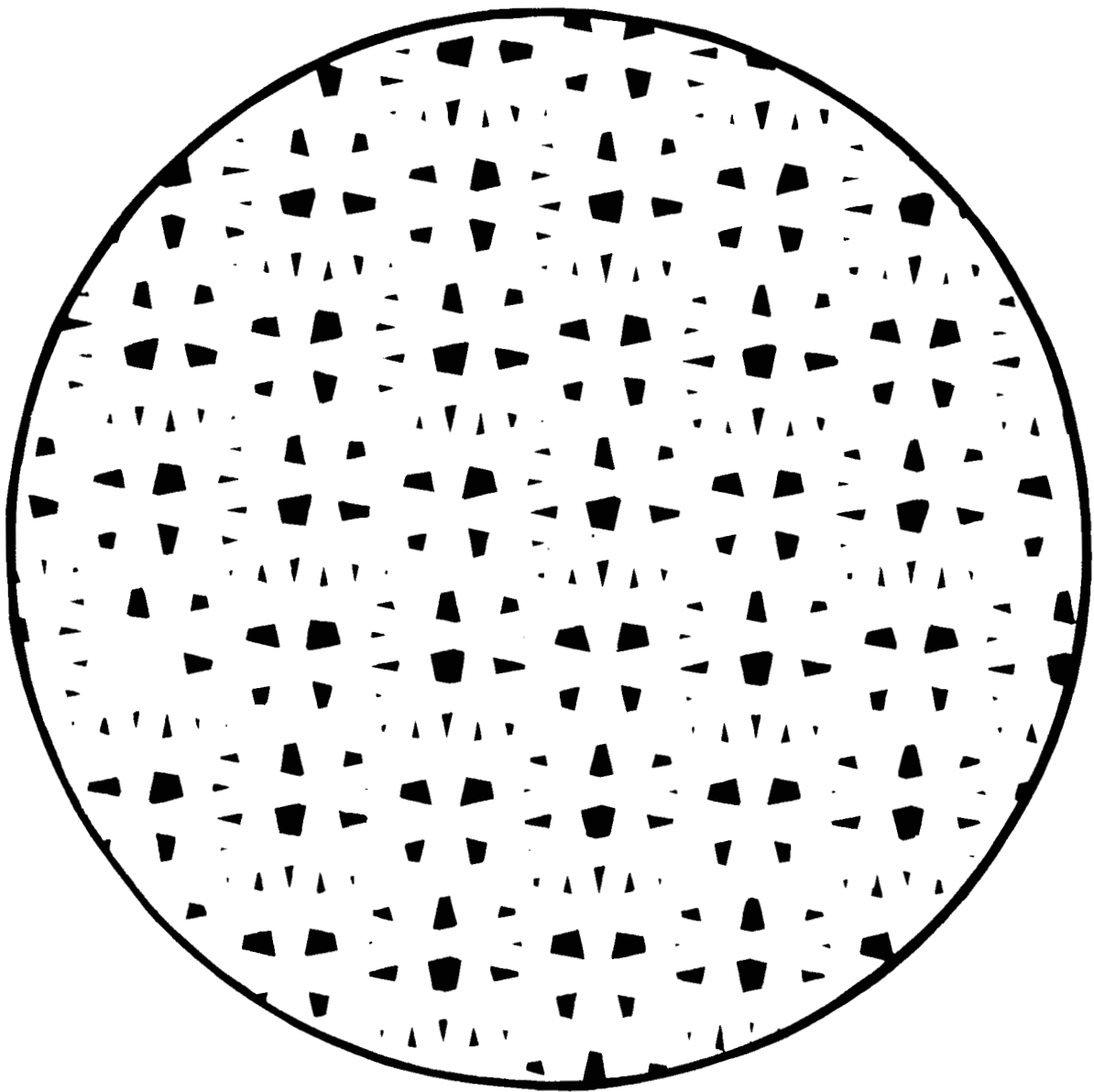
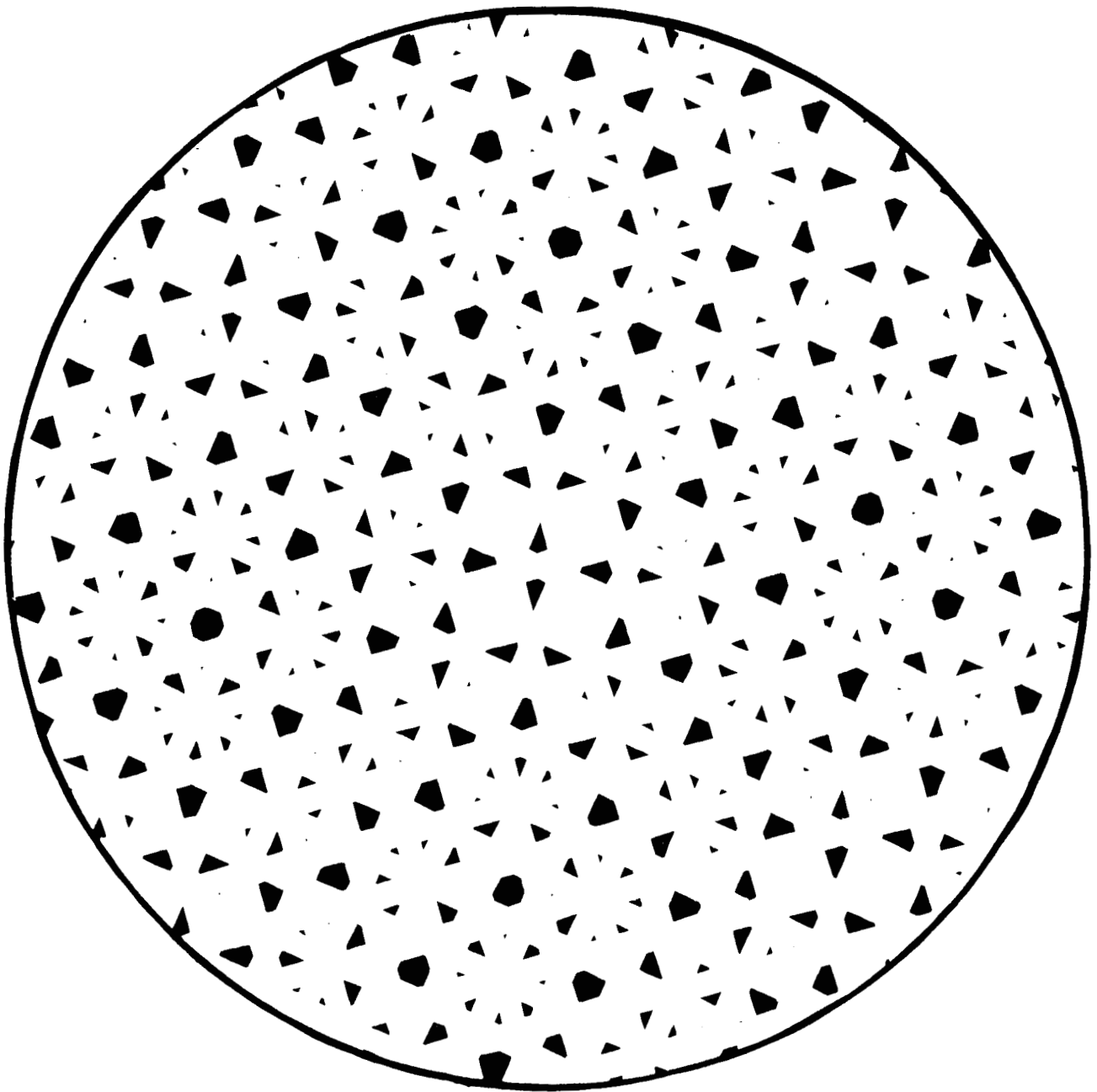FIG. 8 TWO RANDOMLY SUPERIMPOSED SCREENS (OPEN AREA, 0.092)

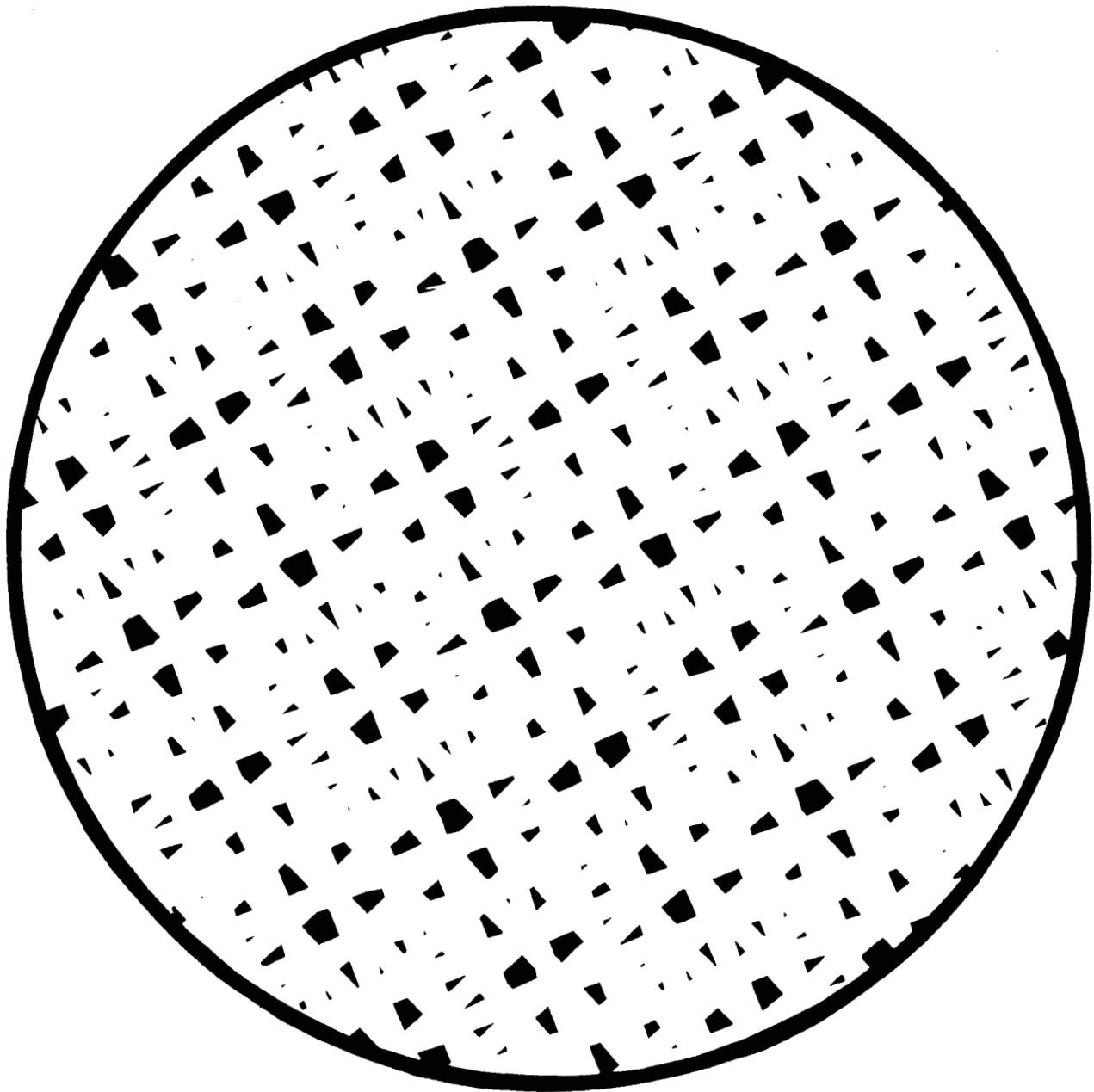FIG. 9   TWO RANDOMLY SUPERIMPOSED SCREENS (OPEN AREA, 0.101)

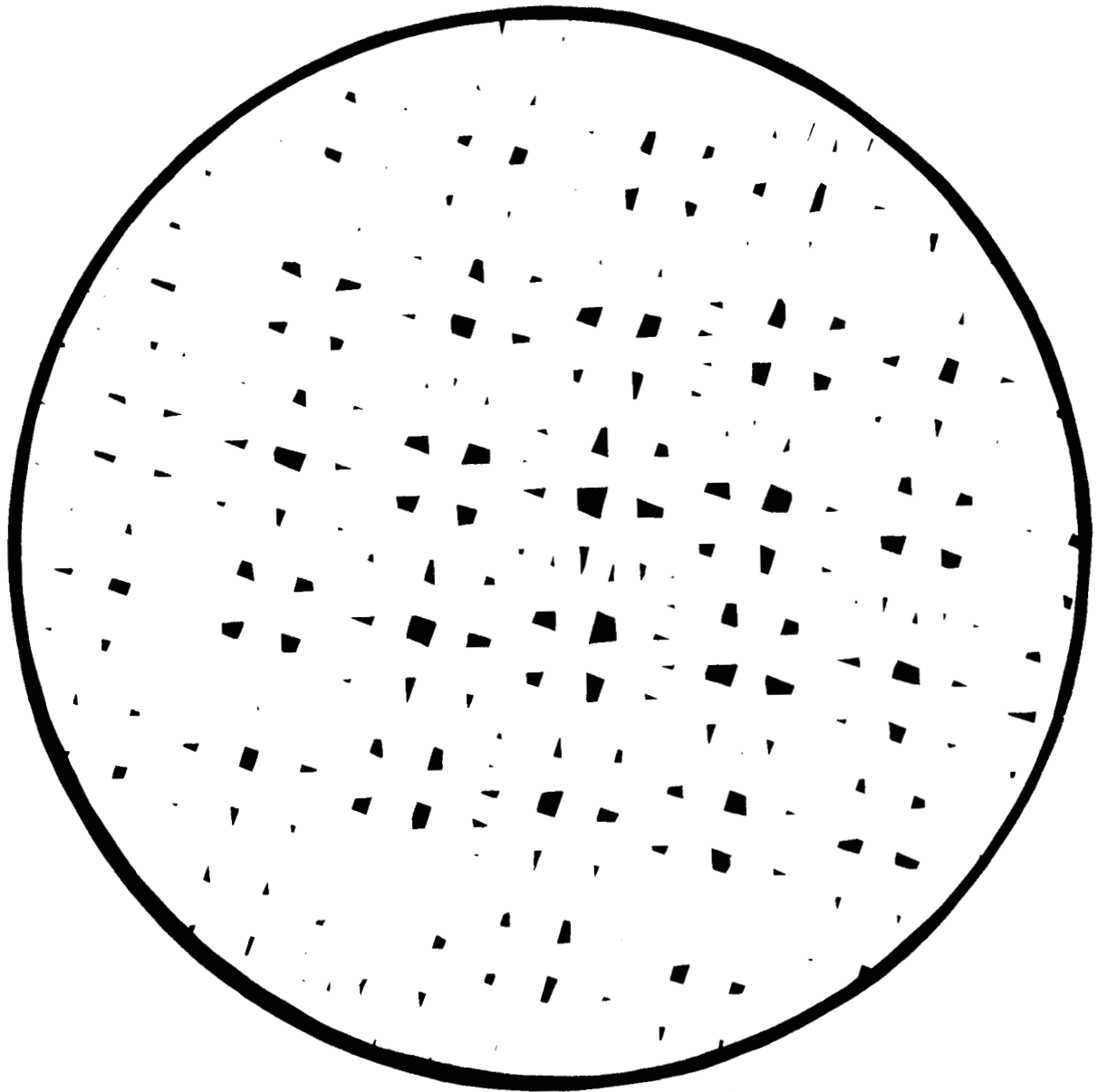FIG. 10 TWO RANDOMLY SUPERIMPOSED SCREENS (OPEN AREA, 0.102)

FIG. II   THREE RANDOMLY SUPERIMPOSED SCREENS
(OPEN AREA, 0.03)

the loss in weight. The predicted open area for these screens was 0.028. The measured open area in two experiments were 0.028 and 0.030, which is in complete accord with predictions within experimental error.

This method of testing the effect of random superposition of screens is cheap, quick, and effective. It is planned to do one more experiment each with three, four, five, six, and finally seven screens. The predicted openings for these values are given in Table 5.

Table 5

FRACTIONAL OPENINGS FOR SEVERAL SUPERIMPOSED SCREENS

Number of Screens	Fractional Open Area
4	0.0070
5	0.0020
6	0.0006
7	0.0002

Therefore, after passing through 7 screens only, 1 photon out of every 5000 would still be travelling in the original direction, even if diffraction effects were completely ignored. This result will be checked by measuring the energy removed from a plane parallel beam of light passed through randomly super-imposed pieces of 325-mesh Tyler screens.

The proportion of open space in the screen studied is 30%, which corresponds to a solids concentration of 70% in a paint film. It can be shown that the area ratio of solid to space exposed on sectioning a composite body is the same as that of the solid to space in the composite body.

Consider the general case of α-percent solids. After n equivalent screens, the percentage area available for straight-through transitions is $(1 - \alpha)^n$. The values for a few values of n and α are given in Table 6.

Table 6
FRACTION OF SPACE AVAILABLE FOR STRAIGHT-THROUGH PASSAGE

α	Number of Equivalent Screens				
	3	4	5	6	7
0.50	0.125	0.062	0.031	0.015	0.007
0.40	0.216	0.130	0.078	0.047	0.028
0.30	0.343	0.240	0.168	0.118	0.083

Table 6 shows that even ignoring diffraction effects after seven screens (which should be equivalent to about seven diameters), 8% of the energy of the incident beam will still persist as a directional element when the film contains 30% solids. The general extension of this treatment and the implications of the data are being pursued.

IIT RESEARCH INSTITUTE

C.   Simulation of Sections through Paint Films

Properties of random screens have been discussed in the preceding section. In applying this theory to paint films, it will be necessary to know the nature of the sections taken through a paint film. Although the average values of the area of the pigment exposed is the same as that of the volume proportion of pigment in the paint formulation, it is necessary to know the fluctuations in the exposed pigment per section. Therefore, we will next describe a Monte Carlo method for simulating sections through a composite body now described. Initially, the simplest case of monosized pigment is considered.

Consider a unit cube that contains N monosized particles. Let the volume concentration of solids be α. Then

$$\alpha = \frac{N}{6} \pi d^3$$

where d is the diameter of the particles.

To simulate the N particles scattered randomly throughout the cube, consider the center of each particle to be specified by coordinates x, y and z drawn from random number tables. The coordinates of the N particles in the x-y plane are plotted on a piece of graph paper, and the particle is represented by a circle on the x-y plane. Since we are considering a random distribution of particles to simulate a random section through the composite, it is sufficient to consider randomly selected x-z planes. To select a plane, a value of y is drawn from

the random number tables. This section appears as a straight line on the x-y plane. This line intersects the circles in the x-y plane, and the length of the intercepts are the diameters of the sections of the particles exposed in the x-z plane. By using this information and the values of the z coordinate, the complete appearance of the x-z section at any value of y can be drawn.

Consider now that we had four sections, as shown in Figure 12. It is assumed that the sections are represented by ink circles on translucent paper. Note in Figure 12B that one circle intercepts the top edge. The missing portion is added to the base of the section to simulate an infinite exposure of solid. Now suppose the value of the solids content is α. To simulate a section through a material of solids concentration 2α, superimpose a upon b and copy the resultant system. Note that since the exposed sections have no symmetry, a can be superimposed on b in four ways by rotating it. Again, since the paper is translucent, it can be inverted and again placed in four possible positions, so that there are eight possible combinations. If we had four sections, it would be possible to simulate 48, $(\frac{4 \times 3 \times 8}{2})$, paired sections for appearance and spatial distribution and six different fractional area exposures. The possibilities of simulation when, for example, twelve different sections are constructed, are very high. If four sections were now placed side by side and reduced photographically to

IITRI-C6018-15
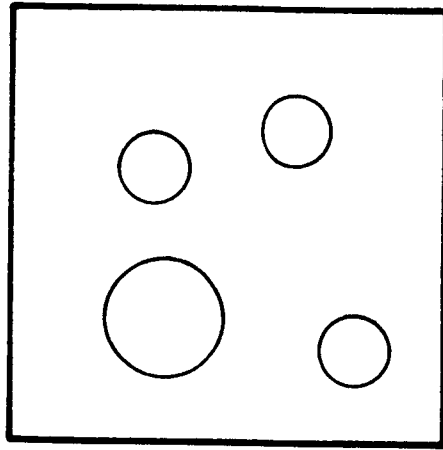
(a)
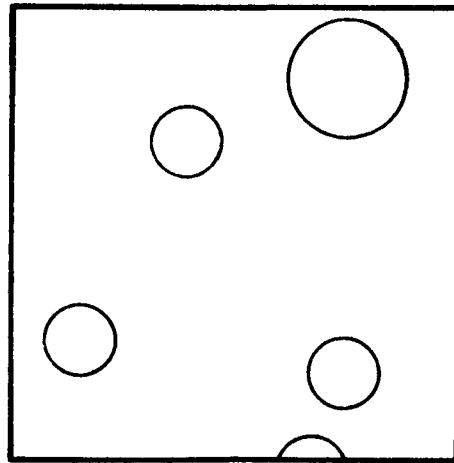
(b)

FIG. 12   SIMULATED SECTIONS THROUGH A PAINT FILM

the size of the original section, this simulates the appearance of a section of the same volume concentration but of one-fourth the particle diameter. Combining this with an original section would simulate twice the concentration of a 1:1 mixture of particles of diameter d and $\frac{d}{4}$.

With relatively few sections, we could simulate sections through composite bodies of various volume concentrations and containing various particle sizes. Although this simulation has been discussed in terms of sections through paint films, the same technique could be used to simulate:

> (1) Various particle-size distributions of particles on a microscope slide. The superposition of a relatively few masters would enable simulation of the appearance of various fields of view, which are random fluctuations about a given real population. This could be particularly useful in evaluating aerial photographs of remote spherical objects or fields of view obtained by using an electron microscope. It would also provide a useful tool for studying overlap losses when particles are deposited on a filter. Since the density of a deposit of air pollution particles is measured photometrically by light reflectance and since particles overlapped are not recorded, this problem is of importance to air pollution studies.

(2) If two masters of the same solids concentration but of different colors are prepared and the two papers then superimposed, the result would represent a section through a mixture of two materials. Again, relatively few masters would enable sections through different mixtures to be simulated. This would provide a fund of experience to enable scientists to decide whether fluctuations observed in a section, e.g., through a propellant mixture or metal alloy, could have arisen by chance in a well-mixed batch or whether they differed sufficiently from possible fluctuations such that segregation within the batch is indicated.

(3) When a composite body is subjected to tensile stress, the maximum stress occurring within the body will be across the plane of minimum plastic element. Thus, in a pigmented plastic, the rupture will occur across the plane with the maximum pigment present. The superimposed masters could be used to simulate experimentally the various possible cross-sections that can occur, the minimum rupture strength predicted, and the patterns of fluctuations established.

It may be possible to patent the simulated sections, because they could have commerical possibilities. They would be particularly useful for training microscopists and for research into properties of composite bodies. Instead of copying superimposed

masters, the masters could be made into slides and projected
directly onto the screen. Simulated sections through paint
films are being constructed. The usefulness of these sections
in predicting the properties of the paints will be explored.

IV. EXPERIMENTAL STUDIES

A. The Optical Properties of Films of Various Thicknesses

A set of monodisperse films of intermediate thickness,
which permitted the measurement of both transmittance and reflectance,
was first prepared. The optical densities of these films are
given in Figure 13. The thickness of the films was measured
interferometrically. The particle radius was 0.30μ (batch 25).
The reflectance measurements of the same films are given in
terms of backscatter intensity in Figure 14. The backscatter
intensity, BI, is calculated from

$$BI = \ln \frac{1}{100 - R_\lambda}$$

where R_λ is the percent reflectance at wavelength λ. The ratio
of backscattered energy to the total scattered energy, called
the backscatter coefficient, is shown in Figure 15.

During the reduction of the data, it was noted that a
linear plot of backscatter intensity, BI, versus ln t, where
t is the film thickness, could be obtained. The data are
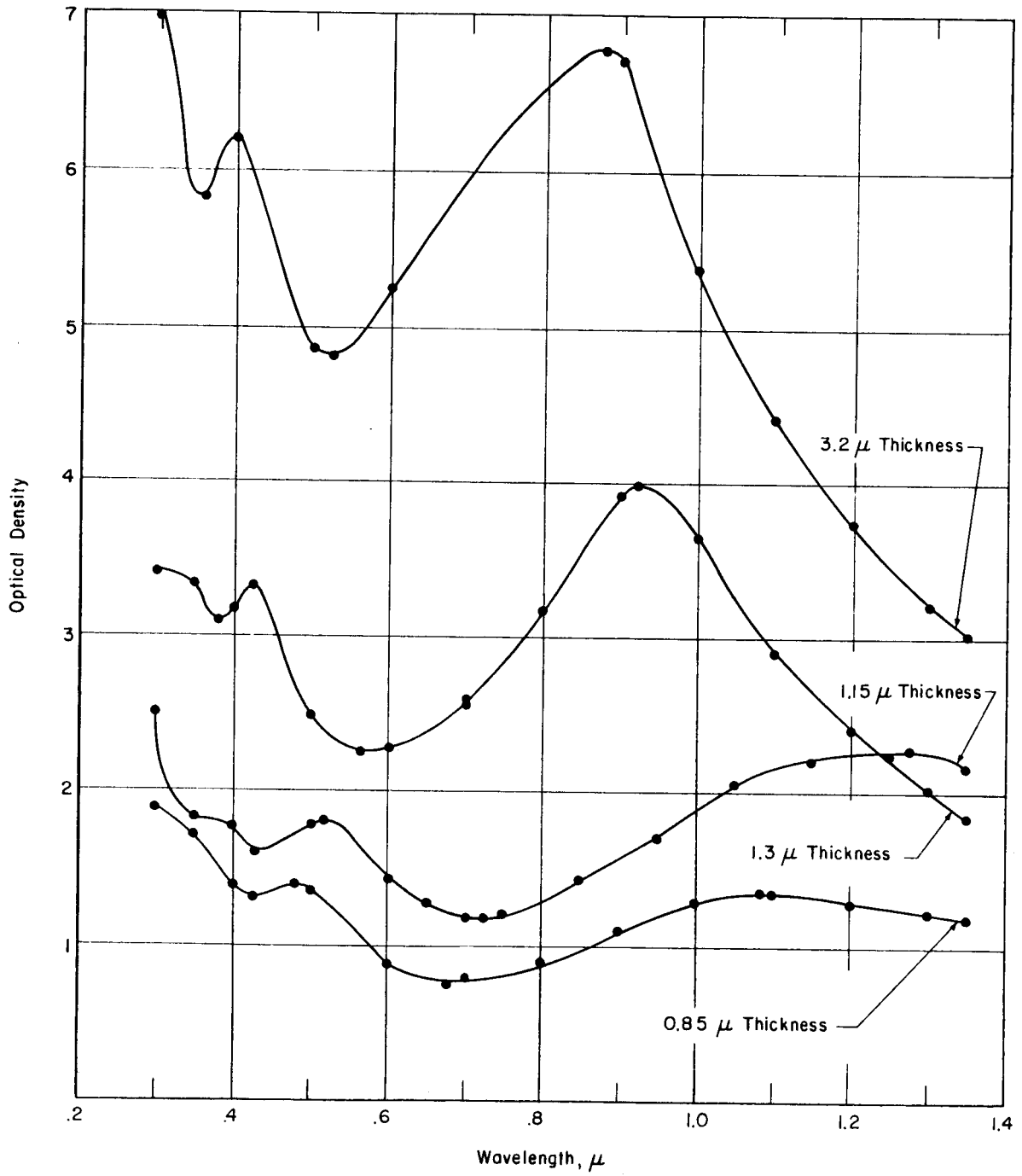presented in Figure 16 for the backscatter intensity at a
wavelength of 0.47μ.
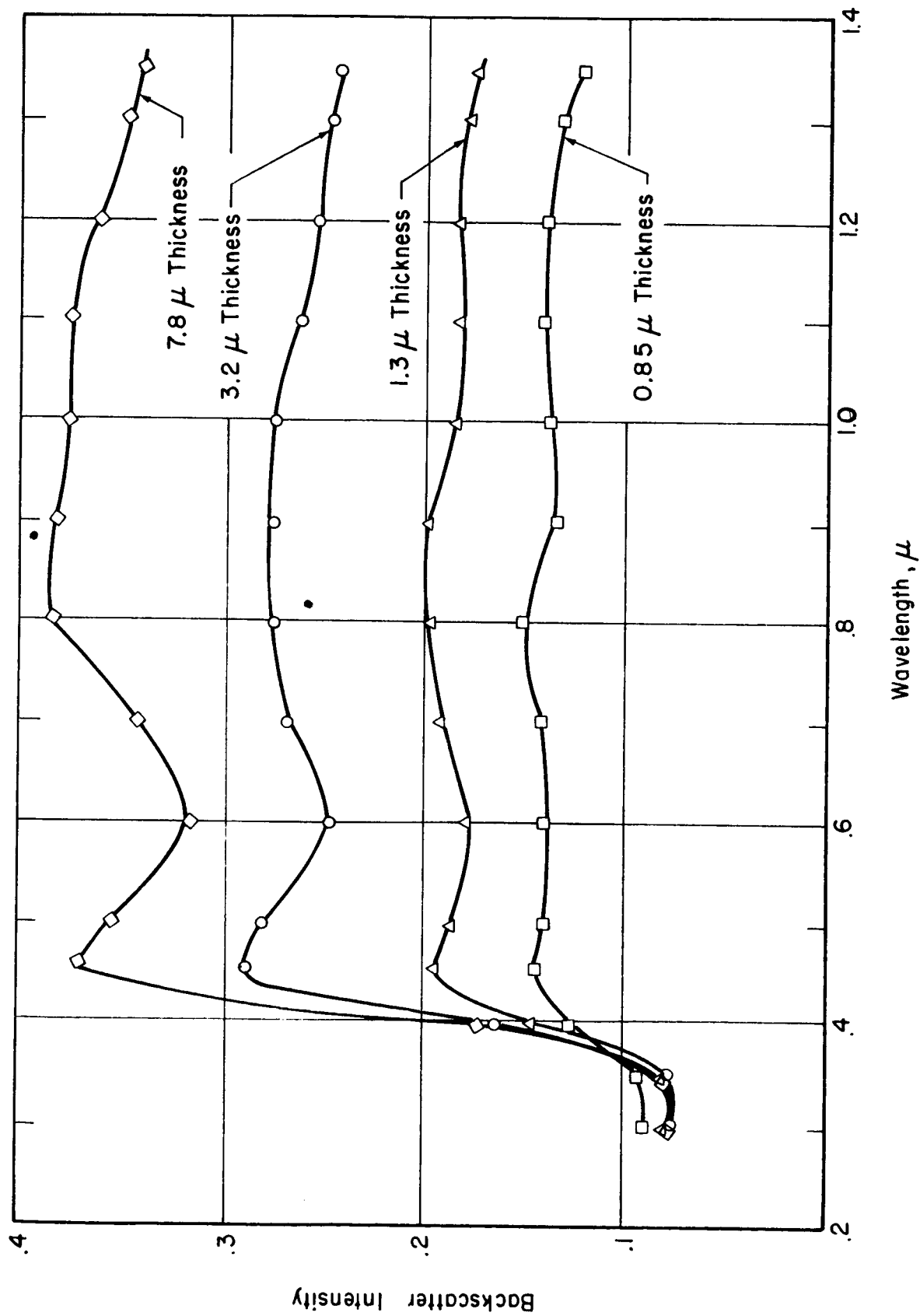
32

FIG. 13   OPTICAL DENSITY WITH VARYING THICKNESS

33

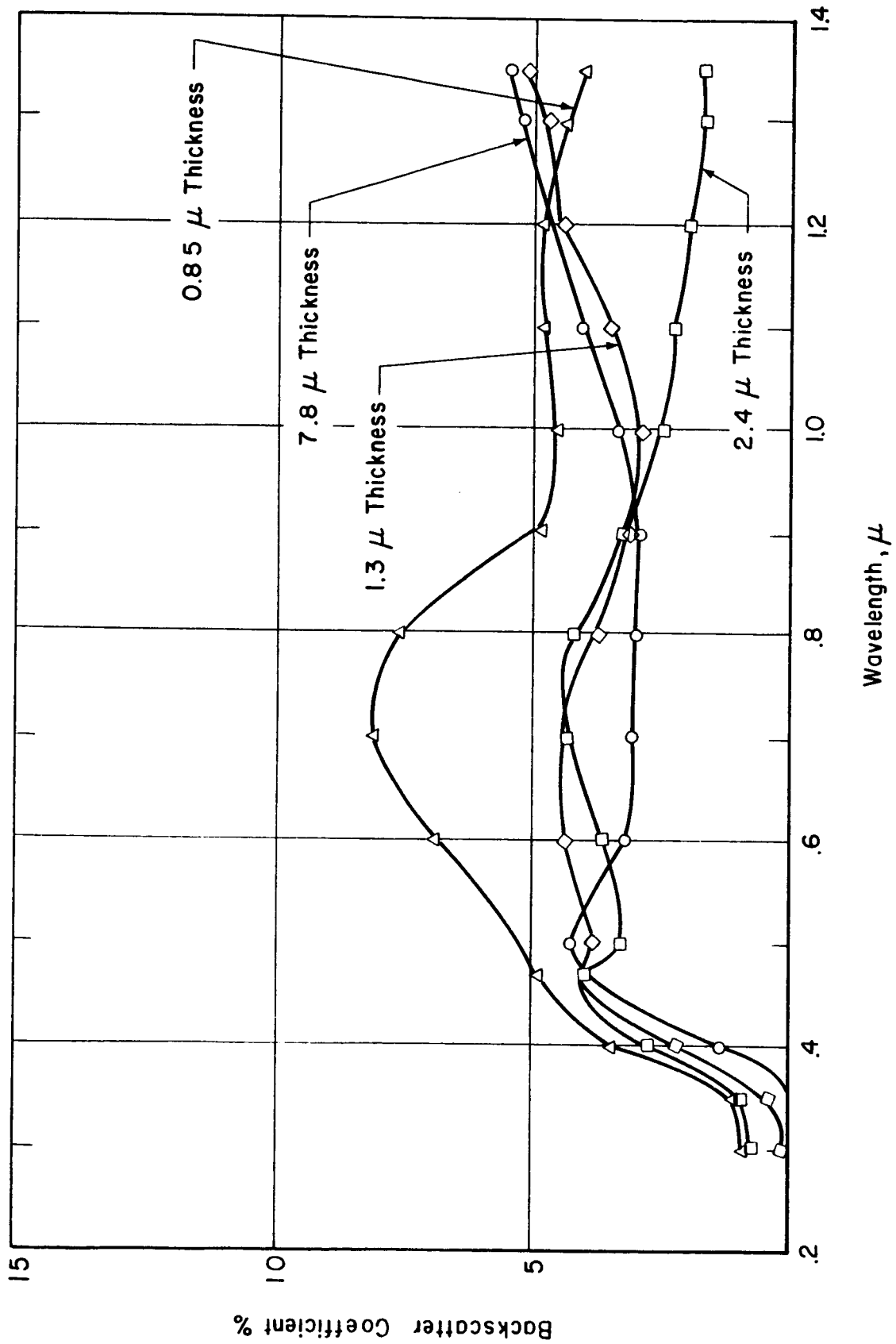FIG. 14 BACKSCATTER INTENSITY WITH VARYING THICKNESS

7.8 μ Thickness

3.2 μ Thickness

1.3 μ Thickness

0.85 μ Thickness

Backscatter Intensity

Wavelength, μ

34

FIG. 15   BACKSCATTER COEFFICIENT WITH VARYING THICKNESS

The chart axes and labels:

- Y-axis: Backscatter Coefficient % (15, 10, 5)
- X-axis: Wavelength, μ (.2, .4, .6, .8, 1.0, 1.2, 1.4)
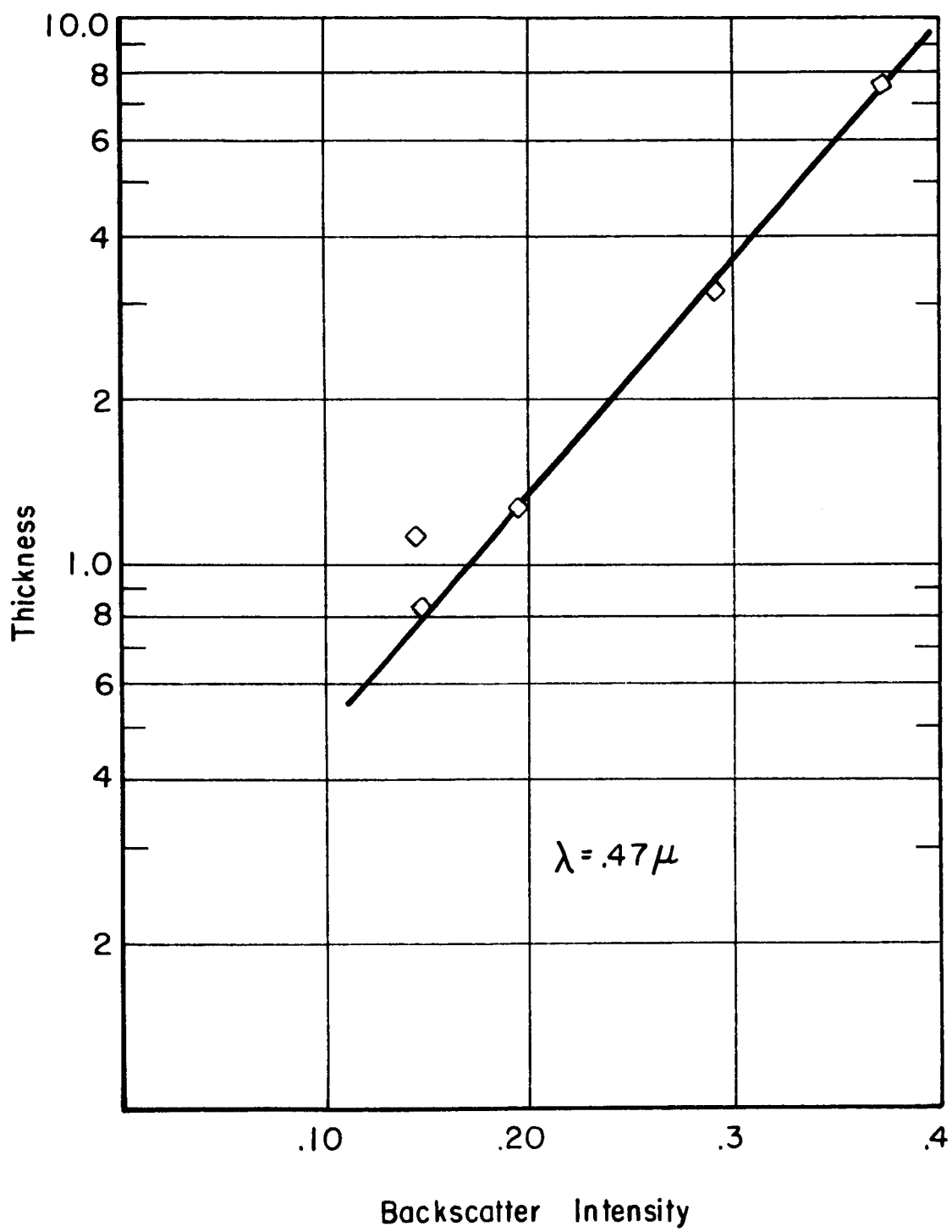- Curve labels: 0.85 μ Thickness, 7.8 μ Thickness, 1.3 μ Thickness, 2.4 μ Thickness

FIG. 16   THICKNESS VS BACKSCATTER INTENSITY (B25)

Additional experiments were performed to confirm the above observation. Two sets of films of various thicknesses were prepared. The thickness of the films was uniform throughout the area of observation. The particle radii were 0.32 μ for barch 26 and 0.20 for batch 30. The reflectances are given in terms of backscatter intensities in Figures 17 and 18. Backscatter intensities at 0.46 μ versus the estimated limits of the thickness measurements for batch 26 are plotted in Figure 19; Figure 20 is a similar plot for batch 30 at a wavelength of 0.45 μ.

Since Figures 16, 19 and 20 are linear plots, the following relationship between reflectance and thickness can be established.

$$\ln \frac{1}{100 - R_\lambda} = C_1 \ln t + \ln C_2 \tag{4}$$

where R_λ is the percent reflectance, t is the film thickness, and C_1 and C_2 are experimental constants corresponding to the slope and the intercept. C_1 and C_2 depend on the particle size, effective refractive index of the system, and the wavelength of measurements. All the given data are at the wavelengths of maximum reflectance (Figures 14, 17 and 18).

Equation 4 can be written as:

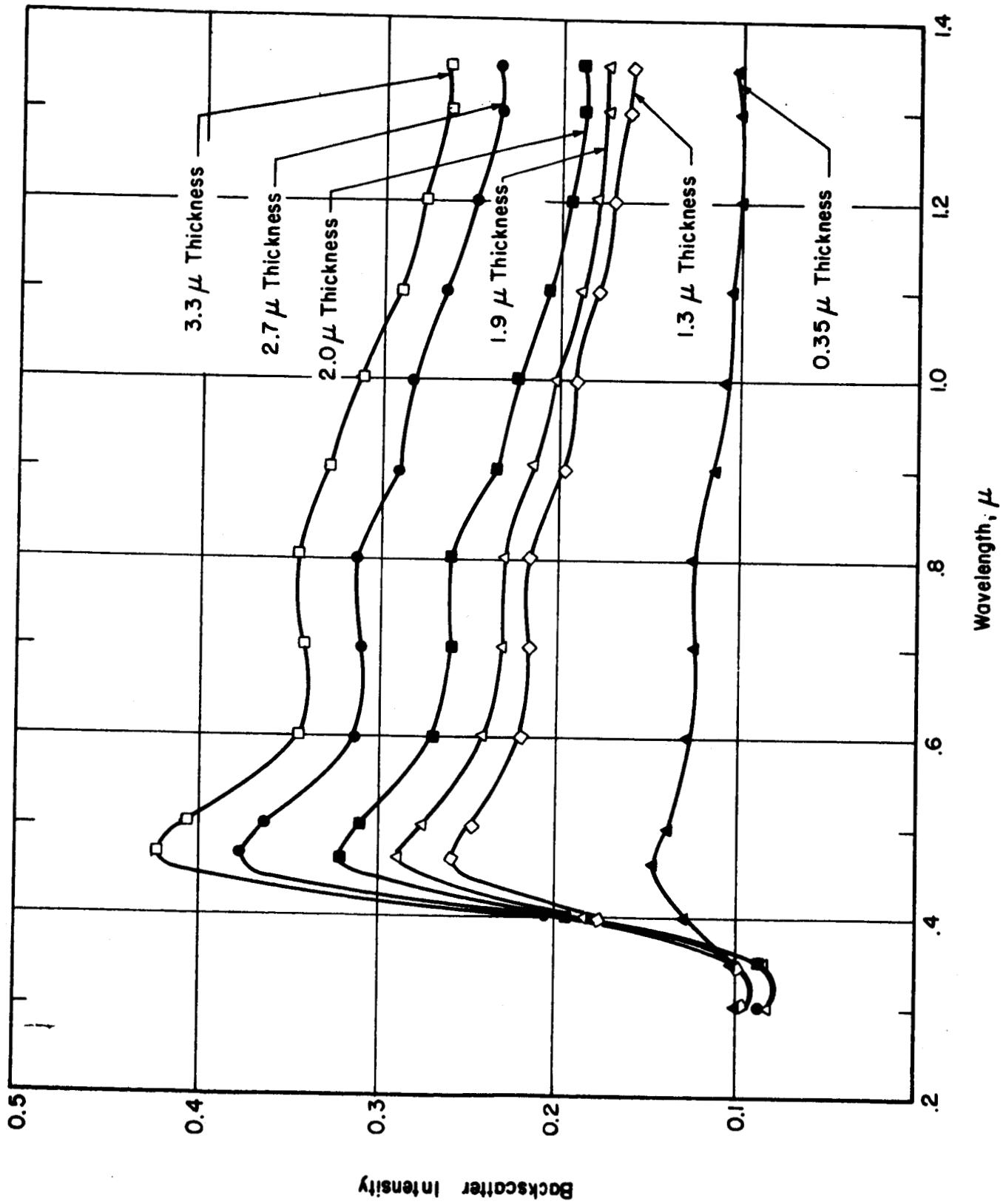$$\frac{1}{100 - R_\lambda} = C_2 t^{C_1} \tag{5}$$

or, in terms of reflectance, R,

30

Backscatter Intensity

Wavelength, μ

FIG. 17   THE BACKSCATTER INTENSITY WITH VARYING THICKNESS (B26)

3.3 μ Thickness
2.7 μ Thickness
2.0 μ Thickness
1.9 μ Thickness
1.3 μ Thickness
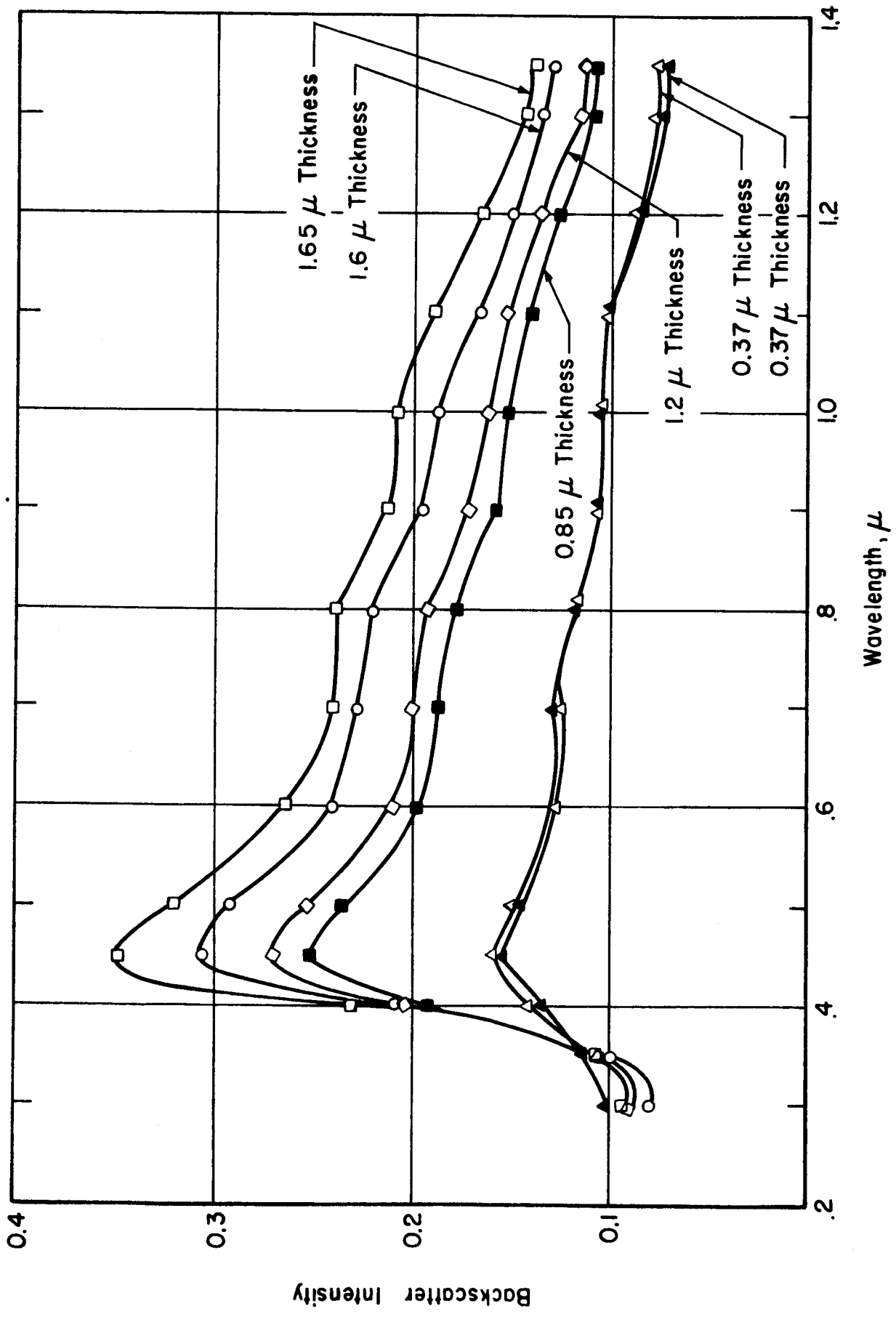0.35 μ Thickness

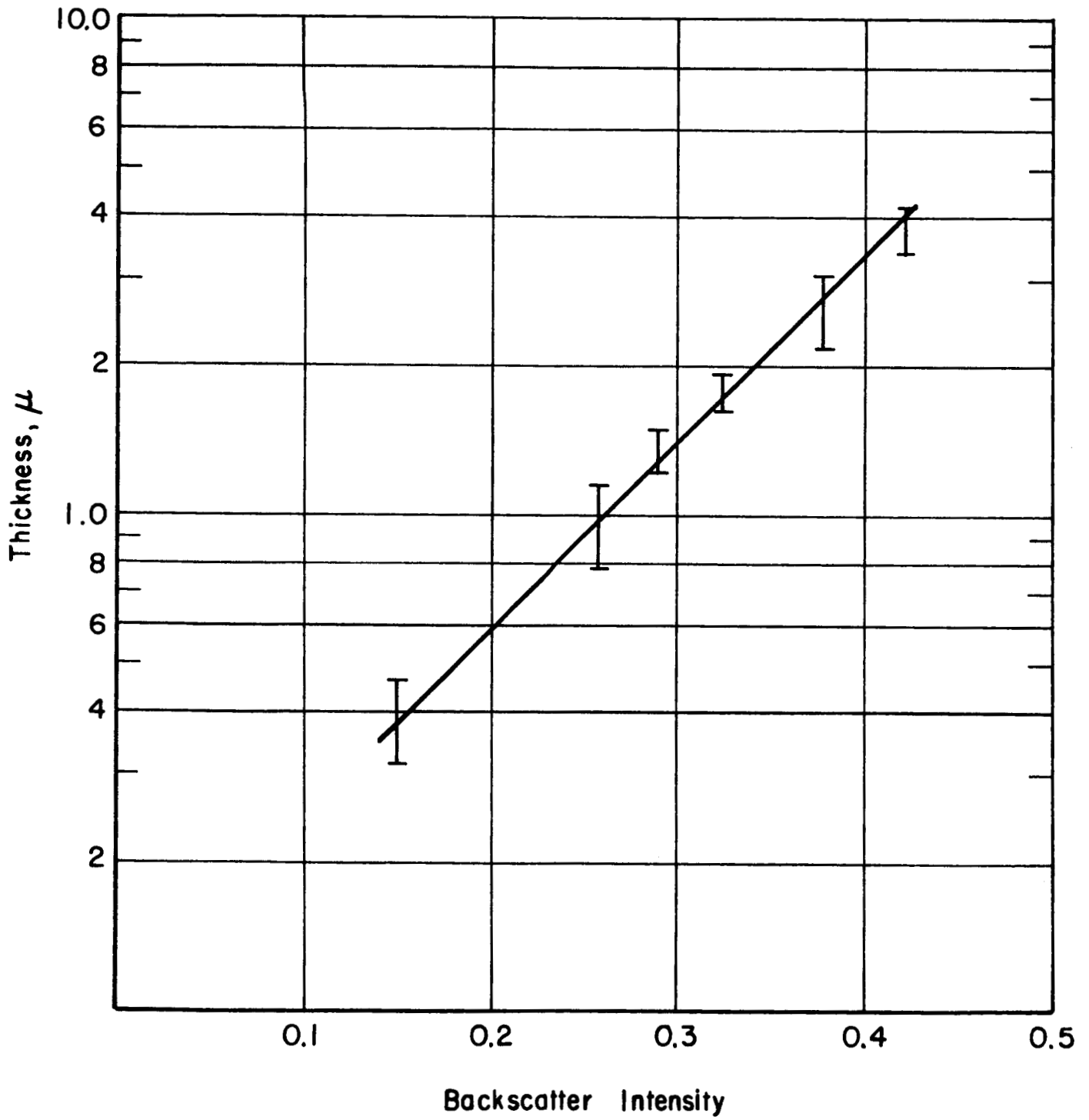FIG. 18 BACKSCATTER INTENSITY WITH VARYING THICKNESS (B30)

40

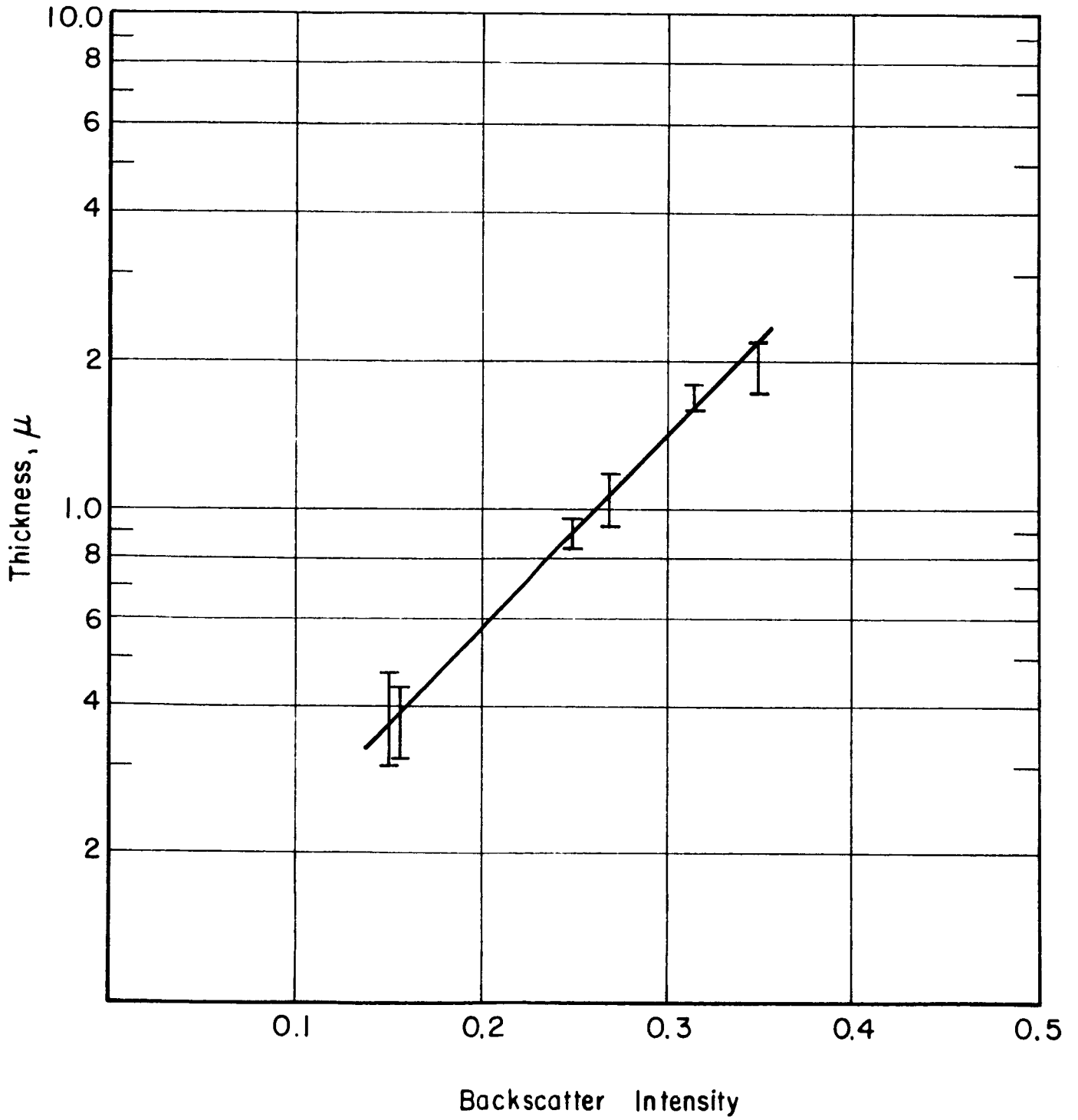FIG. 19   THICKNESS VS BACKSCATTER INTENSITY (B26)

41

FIG. 20 THICKNESS VS BACKSCATTER INTENSITY (B30)

$$R_\lambda = 100 - \frac{1}{c_2 t^{c_1}} \tag{5a}$$

B. The Optical Properties of Flocculated Dispersions

A set of films was prepared from a flocculated suspension
of monodispersed particles. Figure 21 shows the optical density
as a function of wavelength for such a dispersion. The data
show that the oscillations in transmittance have almost disappeared.
Also, the optical density is considerably less than for a well-
dispersed suspension. Figure 22 shows the backscatter coefficient
for this suspension; it indicates a considerable decrease in
backscattering. It is, therefore, concluded that flucculation
tends to destroy the light-scattering properties of monodisperse
films.

C. Discussion of Experimental Studies

The reflectances of thicker films were less than those
of thinner films at wavelengths less than 3.5 μ (Figures 14, 17
and 18). This can be explained on the basis of molecular absorp-
tion of silver bromide. Since at short wavelengths the energy
loss mechanism is absorption and not scattering, the reflectance
of thick films decreases due to increases in the absorptive
path length. It was also noted that the backscatter coefficient
of thin films tends to be slightly higher than that of the
thick ones, and we have previously observed (Report No. IITRI-
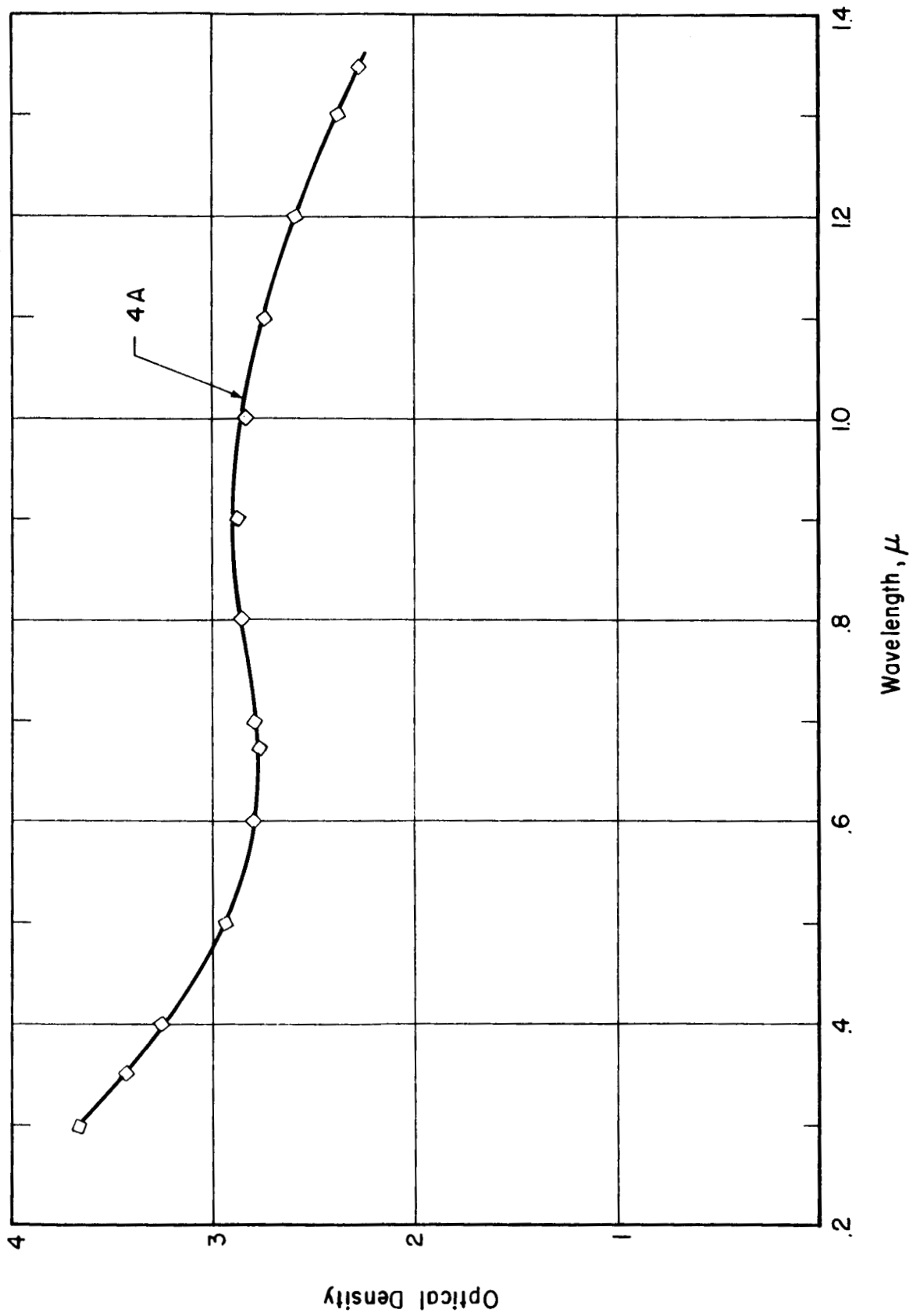C6018-14) that the backscatter intensity obtained from bimodal

IIT RESEARCH INSTITUTE

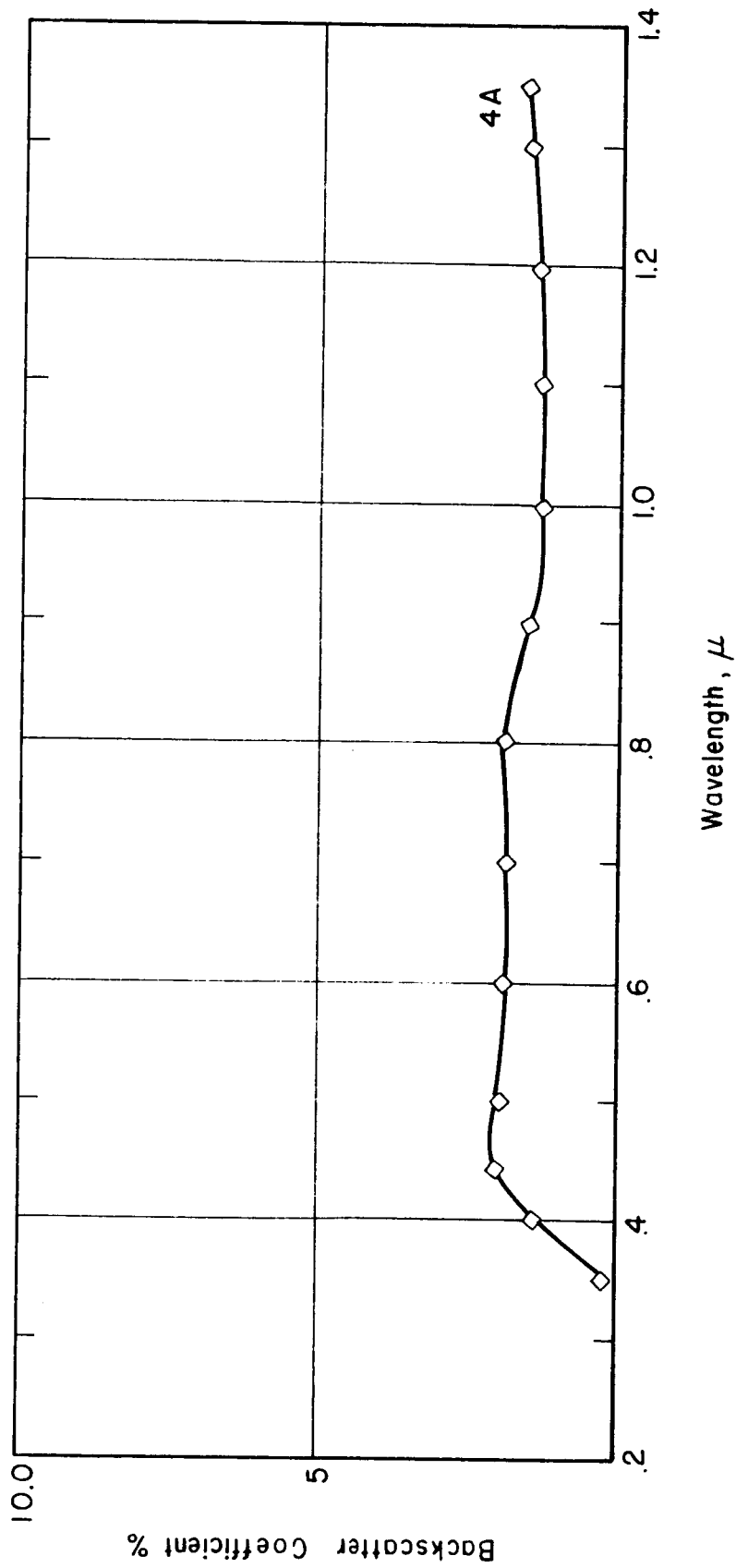FIG. 21 THE OPTICAL DENSITY OF A FLOCCULATED COATING

FIG. 22   THE BACKSCATTER COEFFICIENT AT FLOCCULATED COATING

45

mixtures was less than that predicted from measurements of
monodisperse films. These two observations tend to support
the ideal coating model consisting of thin layers (Report No.
IITRI-C6018-11).

Copy No. _____

Distribution List:

Copy No.	Recipient
1-25 reproducible	National Aeronautics & Space Administration Office of Grants and Research Contracts Washington, D. C.
26	Mr. J. J. Gangler National Aeronautics & Space Administration Office of Advanced Research and Technology Washington 25, D. C.
27-30 + reproducible	Mr. D. W. Gates (M-RP-T) George C. Marshall Space Flight Center Huntsville, Alabama
31	Mr. Conrad Mook Code RV National Aeronautics & Space Administration Washington, D. C.
32	Mr. William F. Carroll Jet Propulsion Laboratory 4800 Oak Grove Drive Pasadena, California
33	Mr. Sam Katzoff National Aeronautics & Space Administration Langley Research Center Langley Field, Virginia
34	Mr. Joseph C. Richmond National Bureau of Standards Washington, D. C.
35 .	Mr. James Diedrich, Mail Stop 7-1 Lewis Research Center Cleveland, Ohio
36	IIT Research Institute Division C Files
37	IIT Research Institute Editors, J. J. Brophy, Main Files
38	IIT Research Institute J. I. Bregman

IIT RESEARCH INSTITUTE

IITRI-C6018-15

Distribution List (cont.)

Copy No.	Recipient
39	IIT Research Institute B. A. Murray
40	IIT Research Institute Y. Harada, Division B
41	IIT Research Institute J. E. Gilligan, Division C
42	IIT Research Institute S. Katz, Division C
43	IIT Research Institute B. Kaye, Division C
44	IIT Research Institute V. Raziunas, Division C
45	IIT Research Institute M. Jackson, Division C
46	IIT Research Institute G. A. Zerlaut, Division C

IIT RESEARCH INSTITUTE

IITRI-C6018-15